2016 IEEE/RSJ International Conference on Intelligent Robots and Systems (IROS)
Daejeon Convention Center
October 9-14, 2016, Daejeon, Korea

Planning Longest Pitch Trajectories for Compliant Serial Manipulators

Sergey A. Kolyubin[1,2] and Anton S. Shiriaev[1]

Abstract— **Our work addresses the problem of planning an optimal pitching trajectory for compliant serial manipulators. We propose a generic framework for finding the longest possible pitch given angle, velocity, and torque constraints. Within this framework we can decompose an original infinite-dimensional task to finite number of similar steps. As a result, the implemented procedure gives an optimal release configuration, temporal control torque profiles satisfying dynamic constraints, and optimal stiffness coefficients for compliant joints. Computational complexity of the nonlinear optimization task was reduced applying a novel motion parametrization method. The proposed method was illustrated for a particular example and experimentally verified with the KUKA LWR4+ arm.**

I. Introduction

Research in pitching optimization is practically motivated, since this kind of dynamic manipulation can increase a working range, optimize power consumption, and shorten an operation cycle time.

In [1] the throwing motion for a 1-DOF planar robot was considered with a special focus on contact dynamics in transition from a finger-link to a fingertip contact. A target-throwing motion was studied in [2] for a 3-DOF fully actuated human-like arm. The aim was to find a trajectory that mimics a baseball pitching motion, when tremendously high speeds in the spherical elbow joint can be reached by low control torques. A different way of programming a dart throwing or a table tennis striking motions based on the reinforcement learning approach has been proposed in [3]. Dynamic manipulation in cluttered environment was described in [4]. A sampled-based planner was implemented ensuring a trajectory passing through a set of intermediate states safely avoiding collisions.

Compliant joints are of special interest for dynamic manipulation studies, because of its ability to store and release energy, which leads to highly-dynamic motions. On the other hand, the presence of compliant joints causes the appearance of proportional number of passive DOFs, which makes motion planning a more complicated task. Indeed, for such systems not only actuation limits, but the dynamics associated with the passive degrees of freedom affects transient behavior.

Such a task has been studied in a number of works. For example, a 2-DOF ball-pitching setup with actuated shoulder and spring-articulated elbow was proposed in [5]. The respective control strategy is based on analysis of zero dynamics arising from a choice of particular geometric synchronization of the generalized coordinates. Similar study is described in [6], where authors analyze effectiveness of the feedback excitation control system in utilizing gravitational and elastic potential energy. Another related study presented in [7], performing human-like golf swings with specified hitting speed at certain impact position. In [8] an alternative approach for a similar two-link pitching robot has been proposed, while the optimization problem was reformulated in discrete time and solved numerically using mathematical programming techniques. For the last years there is also an increasing interest in optimal control of variable-stiffness robots [9], [10]. These works were aimed to propose an approach to simultaneously optimize torque and stiffness temporal profiles to increase dynamic range, agility, and safety of operations, especially involving highly-dynamic motions. To the best of our knowledge most of the works in the field are focused either on heuristic trajectory planning techniques or controller design issues. In contrast, we propose a way to optimize trajectories for underactuated systems based on an analytic criterion.

This question was previously addressed by the authors in [11], [12] considering a two-link underactuated arm. These results illustrate how complexity of a finite-time optimal control problem gets reduced by using a geometric parametrization of motion in the phase space of the system, compared to considering the time evolution of all state variables with respect to an applied input sequence. A necessary condition of optimality and a Lagrangian-type performance index have been derived analytically based on the system's reduced dynamics properties ([13]). Compared to preceding results [11], [12], this work introduces a generic procedure for solving the problem of planning the longest pitch. It shows how the underlying approach can be scaled up for serial manipulators with arbitrary number of degrees of freedom. We also extended the task, performing multi-parametric optimization on release angle and compliant joint stiffness. Moreover, we were able to conduct a series of experiments with the KUKA LWR4+ robotic arm to illustrate the proposed approach and compare simulation and real-life results.

The rest of the paper is organized in the following way. Section 2 describes a generic framework for planning the optimal pitching motion. We will introduce there a step-by-step procedure and propose solutions for motion parametrization, derivation of the performance index and its deviation from the upper bound, multi-parametric constrained optimization and calculation of the initial conditions for that procedure. Finally, in Section 3 we will describe a real-life ball pitching

[1]Sergey Kolyubin and Anton Shiriaev are with the Dept. of Engineering Cybernetics, NTNU, Trondheim, NORWAY
[2] Sergey Kolyubin is also with the Dept. of Control Systems and Informatics, ITMO University, St. Petersburg, RUSSIA {sergey.kolyubin, anton.shiriaev}@ntnu.no

example including implementation issues and comparative analysis of the simulation and experimental results. In conclusions we will underline the most interesting outcomes of the study and discuss several directions for future research.

II. Preliminary Remarks

At first, we will describe a procedure that can be implemented to plan the longest pitch for a serial compliant manipulator given certain kinematic and dynamic constraints. Indeed, this approach is very generic and can be implemented for robots with various kinematics and a number of compliant joints.

A. Problem Formulation and Notations

For clarity of the presentation we introduce here notations for main variables that will be used further in the text.

- $\boldsymbol{q}$, $\dot{\boldsymbol{q}}$, $\ddot{\boldsymbol{q}}$ and $\boldsymbol{\delta}$, $\dot{\boldsymbol{\delta}}$, $\ddot{\boldsymbol{\delta}}$ are vectors of coordinates, velocities, and accelerations of **joints** and **motors** respectively.
- $\boldsymbol{\tau}$ is the vector of control torques.
- $[x, y, z]$ denotes Cartesian coordinates of the end-effector expressed in the 'world' frame.
- $\boldsymbol{\nu} = [\dot{x}, \dot{y}, \dot{z}]^T$ is the vector of linear velocities of the end-effector expressed in the 'world' frame.
- d is the pitching distance calculated from the origin of the 'world' frame.
- ψ is the pitch angle of the coordinate frame attached to the ball grasping device.
- K_s is the vector of the compliant joints' stiffness coefficients.
- indices $(\cdot)_0$ and $(\cdot)_e$ correspond to values of a variable at the pitch starting and release points respectively.
- index $(\cdot)^{opt}$ corresponds to the optimal value of a variable.
- indices $(\cdot)_{min}$ and $(\cdot)_{max}$ correspond to minimum and maximum values of a variable respectively.

The problem addressed here is *how to find a reference trajectory in terms of joint angles, velocities, and accelerations corresponding to the longest possible ball pitch* in a given direction[1].

We consider a ball as a point mass neglecting its rotation. It implies that after its release the ball will experience planar ballistic flight.

The full pitch consists of two phases. The swing phase is when the ball is fixed at the end-effector, and therefore its position can be directly derived as a forward kinematics solution.

Ballistic motion can be described by the following equations

$$\begin{aligned} x(t) =& \dot{x}_e t + x_e, \\ z(t) =& \dot{z}_e t - \frac{g t^2}{2} + z_e, \end{aligned} \tag{1}$$

where $g = 9.81\,[m/s^2]$ is acceleration due to gravity (see Fig. 1).

[1]In this case the 'world' coordinate frame can be always assigned such that its x axis will be aligned with the pitch direction (see Fig. 1)

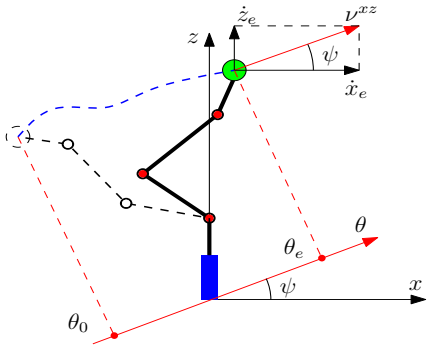

Fig. 1: Schematic sketch for a vertical pitch example

Thus, we can calculate the pitch distance d from (1) as

$$d = x_e + \frac{\dot{x}_e \dot{z}_e}{g} + \dot{x}_e \sqrt{\frac{\dot{z}_e^2}{g^2} + \frac{2 z_e}{g}}. \tag{2}$$

B. Generic Framework

We can split the task of planning the longest pitch on two stages:

1) find $\boldsymbol{q}_e^{opt}$ and $\dot{\boldsymbol{q}}_e^{opt}$ corresponding to the maximum pitching distance (2);
2) find a reference trajectory from $(\boldsymbol{q}_0, 0)$ to $\left(\boldsymbol{q}_e^{opt}, \dot{\boldsymbol{q}}_e^{opt}\right)$ that will satisfy imposed dynamic constraints.

1) Stage 1: In order to calculate d as a function of joint angles $\boldsymbol{q}_e$ and velocities $\dot{\boldsymbol{q}}_e$ at the release point, we derive relations for x_e and z_e from robot forward kinematics, and relations for $\dot{x}_e$ and $\dot{z}_e$ from velocity kinematics

$$\boldsymbol{\nu} = J_\nu(\boldsymbol{q})\dot{\boldsymbol{q}}, \tag{3}$$

where $J_\nu(\boldsymbol{q})$ is the linear velocity Jacobian.

We assume that the grasping device can control ball release direction and extend $\boldsymbol{q}$ with additional rotational DOF q_g that is not actuated during the pitching, i.e. $\dot{q}_g = 0$, but can be adjusted such that $\arctan\left(\frac{\dot{z}_e}{\dot{x}_e}\right) = \psi$, where ψ is the pitch angle that can be uniquely defined for release configuration $\boldsymbol{q}_e$.

Thus, at the first stage we need to solve the following constrained optimization task

$$\max_{\boldsymbol{q}_e^{opt}, \dot{\boldsymbol{q}}_e^{opt}} \left(d(\boldsymbol{q}_e, \dot{\boldsymbol{q}}_e)\right) \quad \texttt{s.t.} \quad \begin{cases} \boldsymbol{q}_e \in [\boldsymbol{q}_{min}; \boldsymbol{q}_{max}], \\ \dot{\boldsymbol{q}}_e \in [\dot{\boldsymbol{q}}_{min}; \dot{\boldsymbol{q}}_{max}], \\ \arctan\left(\frac{\dot{z}_e(\boldsymbol{q}_e, \dot{\boldsymbol{q}}_e)}{\dot{x}_e(\boldsymbol{q}_e, \dot{\boldsymbol{q}}_e)}\right) = \psi. \end{cases} \tag{4}$$

The maximum pitching distance $d^{opt} = d\left(\boldsymbol{q}_e^{opt}, \dot{\boldsymbol{q}}_e^{opt}\right)$ indicates performance that can be reached if we hit physical limits of the robot. At the same time, the solution $(\boldsymbol{q}_e^{opt}, \dot{\boldsymbol{q}}_e^{opt})$ is likely to be non unique, because the same value of d can be reached for different combinations of the release configuration $\boldsymbol{q}_e$ and joint stiffness coefficients K_s.

However, (4) allows to find a global extremum based on kinematics only, and considering similar problem with dynamic constraints gives exactly the same solution.

Velocity of a flexible joint can reach much higher values than its motor velocity $\max|\dot{q}_i| \gg \max\left|\dot{\delta}_i\right|$. Indeed, this is why spring behavior is of interest for highly dynamic manipulation.

Maximum absolute value for velocity of a joint attached by a linear torsional spring can be calculated as

$$\max|\dot{q}_i| = \frac{\max|\tau_i|}{\sqrt{K_s I_i(\boldsymbol{q})}},$$

where $I_i(\boldsymbol{q})$ is its moment of inertia with respect to the axis of rotation, and $\max|\tau_i|$ corresponds to the maximum torque that can be applied to a joint. The latter depends on K_s and its calculation requires dynamics modeling.

On the first stage we use an empiric approach, when compliant joint velocity at the release point is defined as $\dot{q}_e = k\dot{\delta}_e$, where $\dot{\delta}_e$ is the respective motor velocity, and $k > 0$ is the gain. At first, we assign big enough values for k. If later analysis unveils that the selected value of k is infeasible due to system dynamics, optimization (4) should be repeated for smaller k until both optimization stages are consistent.

2) Stage 2: The stage 2 task can be interpreted in the following way. Given optimal release configuration $\boldsymbol{q}_e^{opt}$ and release joint velocities $\dot{\boldsymbol{q}}_e^{opt}$ and assuming that we start from zero velocity $\dot{\boldsymbol{q}}_0 = 0$, find a start configuration $\boldsymbol{q}_0$, stiffness coefficients K_s, and a swing trajectory between $\boldsymbol{q}_0$ and $\boldsymbol{q}_e^{opt}$ that maximizes $|\dot{\boldsymbol{q}}_e|$ and satisfies imposed dynamic constraints[2] .

Accomplishing this task requires in-depth analysis of the underactuated system's dynamics, and a constructive tool for doing that will be introduced in the next section.

If optimization on second stage returns $|\dot{\boldsymbol{q}}_e| < \left|\dot{\boldsymbol{q}}_e^{opt}\right|$ for all possible initial states $(\boldsymbol{q}_0, \boldsymbol{0})$, we can extend pitching backwards with preparatory 'charging' segment(s), until a complete trajectory starting from zero initial velocity will be defined.

III. Optimal Swing Trajectory

A. Motion Parametrization and Optimization Criterion

In order to describe a compliant manipulator dynamics we use the adapted minimalistic model from [9] under similar simplifying assumptions

$$\begin{bmatrix} M(\boldsymbol{q}) & 0 \\ 0 & J(\boldsymbol{q}) \end{bmatrix} \begin{bmatrix} \ddot{\boldsymbol{q}} \\ \ddot{\boldsymbol{\delta}} \end{bmatrix} + \begin{bmatrix} C(\boldsymbol{q}, \dot{\boldsymbol{q}}) & 0 \\ 0 & 0 \end{bmatrix} \begin{bmatrix} \dot{\boldsymbol{q}} \\ \dot{\boldsymbol{\delta}} \end{bmatrix} + \begin{bmatrix} G(\boldsymbol{q}) \\ 0 \end{bmatrix} = \begin{bmatrix} -K_s(\boldsymbol{q} - \boldsymbol{\delta}) \\ K_s(\boldsymbol{q} - \boldsymbol{\delta}) \end{bmatrix} + \begin{bmatrix} 0 \\ \boldsymbol{\tau} \end{bmatrix}, \tag{5}$$

where $M(\boldsymbol{q})$, $C(\boldsymbol{q}, \dot{\boldsymbol{q}})$, and $G(\boldsymbol{q})$ are mass, centrifugal and Coriolis, and gravity forces matrices respectively, $J(\boldsymbol{q})$ is the matrix of motors' inertia. We assume here that elastic elements are linear springs and friction forces are either negligible or compensated by control.

[2]Since $\boldsymbol{\nu}$ in (3) is linear with respect to $\dot{\boldsymbol{q}}$ and assuming that robot Jacobian do not become zeros element-wise, each component in generalized velocities vector $\dot{\boldsymbol{q}}_e^{opt}$ reaches boundary values at maximum $\boldsymbol{\nu}$.

If for n DOFs we have only m compliant joints, (5) can be rewritten in the partitioned form

$$\underbrace{\begin{bmatrix} M_c(\boldsymbol{q}) & 0 & M_{rc}(\boldsymbol{q}) \\ 0 & J_c(\boldsymbol{q}) & 0 \\ M_{rc}^T(\boldsymbol{q}) & 0 & M_r(\boldsymbol{q}) \end{bmatrix}}_{\bar{M}} \begin{bmatrix} \ddot{\boldsymbol{q}}_c \\ \ddot{\boldsymbol{\delta}}_c \\ \ddot{\boldsymbol{q}}_r \end{bmatrix} + \underbrace{\begin{bmatrix} C_c(\boldsymbol{q}, \dot{\boldsymbol{q}}) \\ 0 \\ C_r(\boldsymbol{q}, \dot{\boldsymbol{q}}) \end{bmatrix}}_{\bar{C}} + \underbrace{\begin{bmatrix} G_c(\boldsymbol{q}) \\ 0 \\ G_r(\boldsymbol{q}) \end{bmatrix}}_{\bar{G}} + \underbrace{\begin{bmatrix} K_s(\boldsymbol{q}_c - \boldsymbol{\delta}_c) \\ -K_s(\boldsymbol{q}_c - \boldsymbol{\delta}_c) \\ 0 \end{bmatrix}}_{\bar{K}} = \begin{bmatrix} 0 \\ \boldsymbol{\tau}_c \\ \boldsymbol{\tau}_r \end{bmatrix}, \tag{6}$$

where indices (r), (c), and (rc) correspond to rigid joints, compliant joints, and coupling between dynamics of these two parts respectively, $\boldsymbol{q}_c \in R^m$, $\boldsymbol{\delta}_c \in R^m$, and $\boldsymbol{q}_r \in R^{n-m}$.

The motion parametrization is conventional in optimal trajectory planning, but common approaches can be applied only for fully-actuated systems [14].

Let us introduce a new variable θ called a *path variable* such that joint angles q_i, $i = 1, 2, \dots n$ and motor angles δ_j, $j = 1, 2, \dots m$ can be rewritten as C^2-smooth functions of θ. The requirement for θ is to be monotonically increasing in time. For example, for a planar vertical pitch the path variable can be selected as the projection of the ball coordinate to the axis obtained by rotating the x-axis by the release angle ψ. Fig. 1 illustrates this choice.

The following equations represent geometric relations synchronizing behaviour of motor and joint angles via path variable called *virtual holonomic constraints* (VHC)

$$[\boldsymbol{q}_c, \boldsymbol{\delta}_c, \boldsymbol{q}_r]^T = \Phi(\theta), \tag{7a}$$

and its first and second derivatives

$$[\dot{\boldsymbol{q}}_c, \dot{\boldsymbol{\delta}}_c, \dot{\boldsymbol{q}}_r]^T = \Phi'(\theta)\dot{\theta}, \tag{7b}$$

$$[\ddot{\boldsymbol{q}}_c, \ddot{\boldsymbol{\delta}}_c, \ddot{\boldsymbol{q}}_r]^T = \Phi''(\theta)\dot{\theta}^2 + \Phi'(\theta)\ddot{\theta}, \tag{7c}$$

where

$$\Phi(\theta) = [\phi_1(\theta) \dots \phi_{n+m}(\theta)]^T,$$
$$\Phi'(\theta) = [\partial\phi_1(\theta)/\partial\theta \dots \partial\phi_{n+m}(\theta)/\partial\theta]^T,$$
$$\Phi''(\theta) = [\partial^2\phi_1(\theta)/\partial^2\theta \dots \partial^2\phi_{n+m}(\theta)/\partial^2\theta]^T.$$

Thereby, searching an optimal pitching trajectory $\boldsymbol{q}^\star(t)$ can be reformulated as finding a respective reference trajectory for the path variable $\theta^\star(t)$ on the limited time interval $t \in [0; T]$, where T denotes the swing motion period.

Substituting (7a)–(7c) into (6) and collecting terms with respect to the derivatives of the path variable, we can derive a new representation of the system dynamics

$$\alpha_1(\theta)\ddot{\theta} + \beta_1(\theta)\dot{\theta}^2 + \gamma_1(\theta) = 0, \tag{8a}$$
$$\dots$$
$$\alpha_m(\theta)\ddot{\theta} + \beta_m(\theta)\dot{\theta}^2 + \gamma_m(\theta) = 0, \tag{8b}$$
$$\alpha_{m+1}(\theta)\ddot{\theta} + \beta_{m+1}(\theta)\dot{\theta}^2 + \gamma_{m+1}(\theta) = \tau_{c,1}, \tag{8c}$$
$$\dots$$
$$\alpha_{2m}(\theta)\ddot{\theta} + \beta_{2m}(\theta)\dot{\theta}^2 + \gamma_{2m}(\theta) = \tau_{c,m}, \tag{8d}$$
$$\alpha_{2m+1}(\theta)\ddot{\theta} + \beta_{2m+1}(\theta)\dot{\theta}^2 + \gamma_{2m+1}(\theta) = \tau_{r,1}, \tag{8e}$$
$$\dots$$
$$\alpha_{n+m}(\theta)\ddot{\theta} + \beta_{n+m}(\theta)\dot{\theta}^2 + \gamma_{n+m}(\theta) = \tau_{r,(n-m)}. \tag{8f}$$

The set of first m equations in (8a)-(8f) is of special interest, because there are zeros from the right side. It means that we can not shape solution of this differential equations by control torques. Therefore, for any choice of (7a)–(7c), $\theta^\star(t)$ must simultaneously satisfy solutions of these equations regardless the control strategy implemented.

This way we restrict system dynamics to evolve on a two-dimensional sub-manifold $[\theta, \dot{\theta}] \in R^2$ instead of an original state space $[\boldsymbol{q}, \dot{\boldsymbol{q}}] \in R^{2n}$. It considerably reduces complexity of the optimization task.

Let us illustrate introduced ideas for the case when only one joint is compliant, i.e. $m = 1$. The scalar functions α_1, β_1, and γ_1 in (8a) can be explicitly calculated from (6) and (7a)–(7c) as

$$\alpha_1(\theta) = B^T \bar{M}(\theta)\Phi'(\theta), \tag{9a}$$

$$\beta_1(\theta) = B^T[\bar{M}(\theta)\Phi''(\theta) + \bar{C}(\theta, \Phi'(\theta))\Phi'(\theta)], \tag{9b}$$

$$\gamma_1(\theta) = B^T[\bar{G}(\theta) + \bar{K}(\theta)], \tag{9c}$$

where B is the input matrix annihilator, which can be chosen in our case as $B = [1, 0_{1\times n}]^T$.

As it was shown in [13], solution of (8a) satisfies

$$\dot{\theta}^2(t) = e^{-2\int_{\theta_0}^{\theta(t)} \frac{\beta_1(\tau)}{\alpha_1(\tau)} d\tau} \dot{\theta}_0^2 - \int_{\theta_0}^{\theta} e^{-2\int_{s}^{\theta(t)} \frac{\beta_1(\tau)}{\alpha_1(\tau)} d\tau} \times \frac{2\gamma_1(s)}{\alpha_1(s)} ds. \tag{10}$$

Recalling (7a)–(7c), the task of maximizing $\dot{\boldsymbol{q}}_e$ can be reformulated as $\dot{\theta}_e$ maximization. Therefore, given $\dot{\theta}_0 = 0$, the objective function can be derived from (10)

$$Q = -\int_{\theta_0}^{\theta_e} \left\{ e^{-2\int_{s}^{\theta_e} \frac{\beta_1(\tau, \Phi'(\tau), \Phi''(\tau))}{\alpha_1(\tau, \Phi'(\tau))} d\tau} \times \frac{2\gamma_1(s)}{\alpha_1(s, \Phi'(s))} \right\} ds, \tag{11}$$

where θ_e can be calculated from (7a) for $\boldsymbol{q}_e$.

Remark 1: Any underactuation gives an infinite number of constraints in a form of equalities, i.e. relations that should be valid not point-wise, but along the entire trajectory (see (8a)-(8b)). The proposed approach resolves it automatically, because all trajectories found by maximizing (11) satisfy such constraints, and no additional explicit constraints related to underactuation have to be added to the optimization task formulation.

B. Numerical Optimization

In order to numerically solve the problem of maximizing (11) we approximate VHC by Bézier (or Bernstein) polynomials

$$\phi_1(\theta) = \sum_{k=0}^{N} a_k^1 \frac{N!}{k!(N-k)!} s^k (1-s)^{N-k}, \tag{12}$$

$$\dots$$

$$\phi_{n+m}(\theta) = \sum_{k=0}^{N} a_k^{n+m} \frac{N!}{k!(N-k)!} s^k (1-s)^{N-k},$$

where $s = \frac{\theta - \theta_0}{\theta_e - \theta_0}$, and N is the desired polynomial degree.

Relations (12) is not the only way we can parametrize desired joint trajectories. In general, it could be other kinds of functions that satisfy a requirement on $\phi_i(\theta)$ to be twice differentiable. However, Bézier curves is a natural selection if there is a requirement on smoothness of a generated trajectory. Moreover, (12) enables direct assignment of the release configuration, because $q_e^i = a_N^i$.

Taking into account constraints on joint angles, velocities, torques and its derivatives, we converge to the following constrained optimization problem

$$\max_{\boldsymbol{q}_0, \boldsymbol{a}^1, \dots \boldsymbol{a}^{n+m}, K_s} (Q), \quad \texttt{s.t.} \quad \begin{cases} \boldsymbol{q}_e = \boldsymbol{q}_e^{opt}, \\ \phi_i(\theta) \in [q_{i,min}; q_{i,\max}], \\ \phi_i'(\theta)\dot{\theta} \in [\dot{q}_{i,min}; \dot{q}_{i,\max}], \\ \tau_i(\theta) \in [\tau_{i,min}; \tau_{i,\max}], \\ \dot{\tau}_i(\theta) \in [\dot{\tau}_{i,min}; \dot{\tau}_{i,\max}], \end{cases} \tag{13}$$

where $\boldsymbol{a}^i = [a_0^i, a_1^i \dots a_N^i]$ for $i = 1, 2, \dots n+m$ are coefficient vectors.

Relations for $\tau_i(\theta)$ can be derived solving (8a)–(8b) with respect to $\ddot{\theta}$ and substituting these relations back to (8c)–(8f). At the same time, limits on the joint torque derivatives, which are proportional to jerk, can be defined experimentally. The latter was introduced due to implementation issues. Otherwise, calculated torque profiles can be infeasible to follow for a real robot.

After coefficients in $\boldsymbol{a}^i$, $i = 1, 2 \dots n$ were found, the path variable can be defined from (10) by substituting relations (12) to (7a)–(7c), (9a)–(9c).

In case if a multiple-segment pitch should be planned, target velocity for 'charging' trajectory can be calculated from (7b) for

$$\dot{\theta} = \sqrt{\frac{\left(\dot{\theta}_e^{opt}\right)^2 - Q}{e^{-2\int_{\theta_0}^{\theta_e} \frac{\beta_1(\tau)}{\alpha_1(\tau)} d\tau}}}, \tag{14}$$

where $\dot{\theta}_e^{opt}$ corresponds to $\dot{\boldsymbol{q}}_e^{opt}$.

While the introduced motion planning approach was elaborated for systems with a single passive DOF, the same concept can be implemented for systems with several passive DOFs [15].

IV. Implementation Example

In this section we illustrate how the proposed optimal trajectories planning approach can be implemented considering an example of planar vertical pitch performed by KUKA LWR4+ serial redundant manipulator (LWR).

A. Setup Description

For the vertical pitch experiment we kept axes *A1, A4, A6,* and *E1* fixed by feeding constant values as reference positions. Joints *A2* and *A3* were considered to be rigid, while the the wrist joint *A5* was considered as a compliant one (see Fig. 2a).

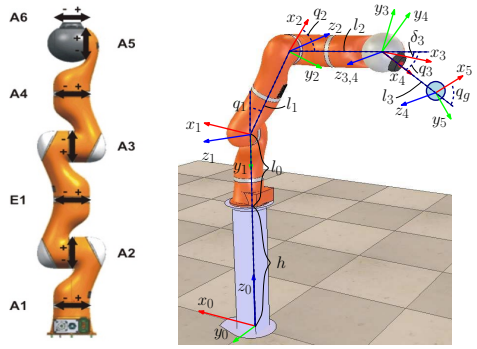

(a) Axes labelling (b) Kinematic sketch

Fig. 2: Experimental setup

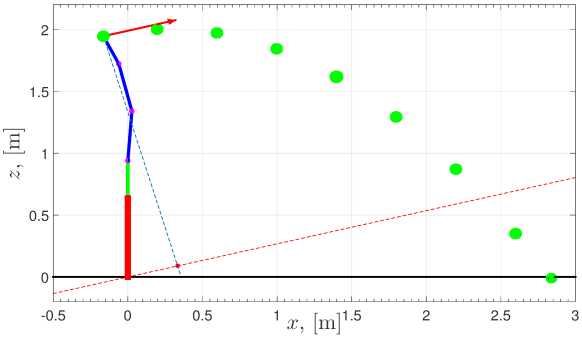

Fig. 3: Optimal release configuration and simulated ballistic trajectory

Thus, we deal with a planar serial manipulator with two rigid rotational joints q_1, q_2 and one elastic joint characterized by 2 DOFs, i.e. motor angle δ_3 and joint angle q_3. We assigned joint coordinate frames satisfying Denavit-Hartenberg (DH) convention (see Fig. 2b).

In this case the end-effector's Cartesian coordinates can be calculated as

$$\begin{aligned} x =& l_1\cos(q_1) + l_2\cos(q_1+q_2) \\ &+ l_3\cos(q_1+q_2+q_3), \\ z =& h + l_0 + l_1\sin(q_1) + l_2\sin(q_1+q_2) \\ &+ l_3\sin(q_1+q_2+q_3). \end{aligned} \tag{15}$$

If we select the path variable as illustrated in Fig. 1 it can be calculated as

$$\begin{aligned} \theta =& l_1\cos(q_1-\psi) + l_2\cos(q_1+q_2-\psi) \\ &+ l_3\cos(q_1+q_2+q_3-\psi). \end{aligned} \tag{16}$$

Values for DH-parameters θ_i, d_i, a_i, and α_i are given in [16].

For the given example we need to introduce only three Bézier polynomial approximations for VHC

$$\begin{aligned} q_1(\theta) &= \phi_1(\theta) = \sum_{k=0}^{N} a_k^1 \frac{N!}{k!(N-k)!} s^k (1-s)^{N-k}, \\ q_2(\theta) &= \phi_2(\theta) = \sum_{k=0}^{N} a_k^2 \frac{N!}{k!(N-k)!} s^k (1-s)^{N-k}, \\ \delta_3(\theta) &= \phi_3(\theta) = \sum_{k=0}^{N} a_k^3 \frac{N!}{k!(N-k)!} s^k (1-s)^{N-k}. \end{aligned} \tag{17}$$

To find a VHC for $q_3(\theta)$ we substitute (17) to (16) and resolve it with respect to q_3.

LWR dynamic parameters have been identified using the approach described in [17]. This is a separate study and its details and results are not reported in this paper due to limited space.

Because of the safety considerations LWR does not allow exceeding joint velocity limits even if it was actuated in a compliant mode. Therefore, while planning the longest pitch, we put constraints on all joints velocities as well. If a physical spring were introduced, e.g. similar to variable stiffness actuators (see [9], [10]), our approach provides a tool for employing power of compliance in generating explosive motions. However, in this study we set a goal to investigate boundaries of LWR's performance. Values for the imposed constraints can be checked from [16].

To command the robot via *'Fast Research Interface'* (FRI) we used an open-source Stanford FRI library (see [18]). LWR was operated in the *'Joint Impedance Control'* mode, when the commanded torque is calculated as

$$\tau_{cmd} = K_s(q - q_{msr}) + D(\xi) + f_{dyn} + \Delta\tau,$$

where $q^\star$ and q_{msr} are reference and measured joint angles respectively, $D(\xi)$ is the damping terms, ξ is the normalized damping ratio, f_{dyn} is the dynamics compensation term that in the activated mode takes into account only the current robot gravity vector $f_{dyn} = G(q_{msr})$, and $\Delta\tau$ is the commanded torque offset that can be defined by the user in an arbitrary way. For rigid joints we set the maximum allowed stiffness of 2000 Nm/rad and relied on tracking performance of the LWR native controller. At the same time, for the compliant joint we tried to implement 'pure torque' control, i.e. zeroed the stiffness coefficient and calculated the torque offset as

$$\Delta\tau = -D(\xi) - G(q_{msr}) + \tau_c,$$

where τ_c is the torque reference along the optimized pitch trajectory calculated from the identified model. Values for $G(q_{msr}$ were obtained on-line using the *'GetCurrentGravityVector'* function.

B. Simulation and Experimental Results

The optimal release configuration for the planar vertical pitch found on stage 1 and the ball ballistic motion after its release are illustrated in Fig. 3.

Resulting characteristics of the experimentally verified pitch can be found in [16]. Figures 4a–4c show evolution of joint angles, velocities, and torques along the pitching trajectory. These plots compare simulated and real motions.

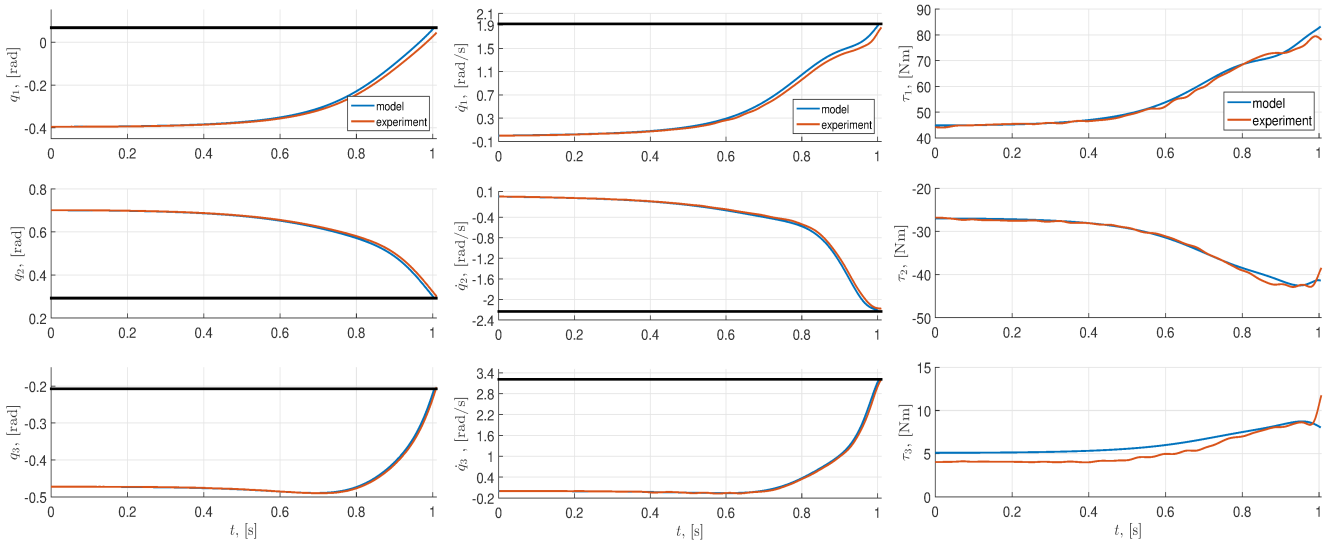

(a) Joint angles (b) Joint velocities (c) Joint torques

Fig. 4: Comparison of the simulated reference trajectory and experimental results for planar vertical pitch (bold black horizontal lines show respective limits)

V. Discussion and Future Work

We introduced a generic framework for planning the longest pitch by serial compliant manipulators. Results of the proposed procedure include an optimal release configuration $\boldsymbol{q}_e$, reference trajectory $\boldsymbol{q}^\star(t)$ satisfying imposed dynamic constraints, and optimal stiffness coefficients K_s for compliant joints.

It gives a constructive tool for finding reference trajectories for robots with weakly or underactuated joints such that these trajectories satisfy a certain analytic optimization criterion and imposed dynamic constraints. It also has no principal limits to be implemented for serial manipulators with arbitrary number of degrees of freedom and sophisticated motions. We successfully conducted several experiments with the KUKA LWR4+ robotic arm to illustrate the proposed approach and compare simulation and real-life results.

The proposed approach can be also adapted for variable stiffness actuators, when joint compliance can be adjusted along a trajectory.

References

[1] W. Mori, J. Ueda, and T. Ogasawara, "1-DOF dynamic pitching robot that independently controls velocity, angular velocity, and direction of a ball: Contact models and motion planning," in *Proc. IEEE ICRA '09*, May 2009, pp. 1655–1661.

[2] T. Senoo, A. Namiki, and M. Ishikawa, "High-speed throwing motion based on kinetic chain approach," in *Proc. IEEE/RSJ IROS '08*, Sep. 2008, pp. 3206–3211.

[3] J. Kober, A. Wilhelm, E. Oztop, and J. Peters, "Reinforcement learning to adjust parametrized motor primitives to new situations," *Autonomous Robots*, vol. 33, no. 4, pp. 361–379, Apr. 2012.

[4] Y. Zhang, J. Luo, and K. Hauser, "Sampling-based motion planning with dynamic intermediate state objectives: Application to throwing," in *Robotics and Automation (ICRA), 2012 IEEE International Conference on*, May 2012, pp. 2551–2556.

[5] S. Ichinose, S. Katsumata, S. Nakaura, and M. Sampei, "Throwing motion control experiment utilizing 2-link arm passive joint," in *Proc. SICE Annual Conference*, Aug. 2008, pp. 3256–3261.

[6] T. Hondo and I. Mizuuchi, "Design and modal analysis of feedback excitation control system for vertical series elastic manipulator," in *Proc. IEEE/RSJ IROS' 13*, Nov. 2013, pp. 2888–2893.

[7] C. Xu, A. Ming, T. Nagaoka, and M. Shimojo, "Motion control of a golf swing robot," *J. Intell. Rob. Syst.*, vol. 56, no. 3, pp. 277–299, 2009.

[8] E. L. Yedeg and E. Wadbro, "State constrained optimal control of a ball pitching robot," *Mech. Mach. Theory*, vol. 69, pp. 337–349, 2013.

[9] D. Braun, F. Petit, F. Huber, S. Haddadin, P. van der Smagt, A. Albu-Schaffer, and S. Vijayakumar, "Robots driven by compliant actuators: Optimal control under actuation constraints," *IEEE Trans. Robot.*, vol. 29, no. 5, pp. 1085–1101, Oct. 2013.

[10] M. Garabini, A. Passaglia, F. Belo, P. Salaris, and A. Bicchi, "Optimality principles in variable stiffness control: The vsa hammer," in *Proc. IEEE/RSJ IROS '11*, Sep. 2011, pp. 3770–3775.

[11] U. Mettin, A. Shiriaev, L. Freidovich, and M. Sampei, "Optimal ball pitching with an underactuated model of a human arm," in *Proc. IEEE ICRA '10*, May 2010, pp. 5009–5014.

[12] U. Mettin and A. Shiriaev, "Ball-pitching challenge with an underactuated two-link robot arm," in *Proc. 18th IFAC World Congress*, Aug. 2011, pp. 11 399–11 404.

[13] A. Shiriaev, J. Perram, and C. Canudas-de Wit, "Constructive tool for orbital stabilization of underactuated nonlinear systems: Virtual constraints approach," *IEEE Trans. Aut. Control*, vol. 50, no. 8, pp. 1164–1176, Aug. 2005.

[14] J. Bobrow, S. Dubowsky, and J. Gibson, "Time-optimal control of robotic manipulators along specified paths," *The Int. J. of Rob. Research*, vol. 4, no. 3, pp. 3–17, Sep. 1985.

[15] P. X. M. L. Hera, A. S. Shiriaev, L. B. Freidovich, U. Mettin, and S. V. Gusev, "Stable walking gaits for a three-link planar biped robot with one actuator," *IEEE Trans. Robot.*, vol. 29, no. 3, pp. 589–601, Jun. 2013.

[16] "Appendix. data tables." [Online]. Available: https://www.dropbox.com/s/ygyv9ogb9zpnyei/KolyubinIROS16App.pdf

[17] A. Jubien, M. Gautier, and A. Janot, "Dynamic identification of the Kuka LWR robot using motor torques and joint torque sensors data," *IFAC Proceedings Volumes (IFAC-PapersOnline)*, vol. 19, pp. 8391–8396, 2014.

[18] "Fast research interface library." [Online]. Available: http://cs.stanford.edu/people/tkr/fri/html/index.html